Advances and Applications in Fluid Mechanics
© 2023 Pushpa Publishing House, Prayagraj, India
http://www.pphmj.com
http://dx.doi.org/10.17654/0973468623003
Volume 30, Number 1, 2023, Pages 35-62 **ISSN: 0973-4686**

NUMERICAL STUDY OF BIOMAGNETIC FLUID FLOW OVER AN UNSTEADY CURVED STRETCHING SHEET IN THE PRESENCE OF MAGNETIC FIELD

M. G. Murtaza[1], Tamanna Akter[1], E. E. Tzirtzilakis[2] and M. Ferdows[3,*]

[1]Department of Mathematics
Comilla University
Cumilla-3506
Bangladesh
e-mail: limonn@yahoo.com
tamannaaktercou31@gmail.com

[2]Fluid Mechanics and Turbomachinery Laboratory
Department of Mechanical Engineering
University of the Peloponnese
Tripoli, Greece

Received: January 7, 2023; Accepted: February 21, 2023

2020 Mathematics Subject Classification: 92C10, 80A50, 76D10, 76D05, 76W05.

Keywords and phrases: biomagnetic fluid, magnetic dipole, curved stretching sheet, finite difference method.

[*]Corresponding author

How to cite this article: M. G. Murtaza, Tamanna Akter, E. E. Tzirtzilakis and M. Ferdows, Numerical study of biomagnetic fluid flow over an unsteady curved stretching sheet in the presence of magnetic field, Advances and Applications in Fluid Mechanics 30(1) (2023), 35-62. http://dx.doi.org/10.17654/0973468623003

Published Online: March 6, 2023

[3]Research Group of Fluid Flow Modeling and Simulation
Department of Applied Mathematics
University of Dhaka
Dhaka-1000, Bangladesh
e-mail: ferdows@du.ac.bd

Abstract

The aim of this paper is to analyze the biomagnetic fluid flow - namely the flow of blood over an unsteady curved stretching sheet in the presence of magnetic field. This study emphasizes the effect of ferrohydrodynamics (FHD) interaction parameters on the flow field and FHD has a great enhancement effect on biomagnetic fluid rather than regular fluid. The complicated coupled system of differential equations that is the leading equations of continuity, momentum and energy equations are converted into non-dimensional form with some suitable similarity variables. This solution is obtained numerically by applying an efficient numerical technique based on finite difference method, consisting of central differencing, tridiagonal matrix manipulation and an iterative procedure. By using Fortran software, the solution of the nonlinear problem is produced. The obtained numerical values are plotted through graphs for velocity, temperature dimensionless pressure, skin friction coefficient, rate of heat transfer (local Nusselt number) and dimensionless wall pressure with various parameters, and the variations based on these plots are discussed. The obtained results reveal that the dimensionless velocity is increased considerably with the increment of ferromagnetic interaction parameter and stretching parameter whereas temperature profile and dimensionless pressure show inverse relation. Both fluid velocity and temperature profiles decrease with the increasing value of curvature and suction parameters and reverse trend is true for dimensionless pressure. It is also incurred that the skin friction coefficient, rate of heat transfer and dimensionless wall pressure increase with the increasing value of curvature parameter. Finally, the accuracy of the results is also compared for some specific values of the parameters with other documented in literature, and the results are found to be in good agreement.

Nomenclature

η	Similarity variable
$(u,\ v)$	Velocity components (ms^{-1})
$(s,\ r)$	Spatial coordinate (m)
P	Fluid pressure (kg/ms^2)
M_1	Magnetization (A/m)
H	Magnetic field intensity (A/m)
T	Fluid temperature inside the boundary layer (K)
T_∞	Dimensionless ambient temperature (K)
T_w	Dimensionless surface temperature at the wall (K)
Re	Reynolds number
Re_s	Local Reynolds number
θ	Dimensionless temperature
ψ	Dimensionless stream function
ρ	Density of fluid (kg/ms^3)
μ	Dynamic viscosity (kg/ms)
ν	Kinematic viscosity (m^2/s)
α'	Thermal diffusivity (m^2/s)
μ_0	Magnetic permeability ($Kg.m/A^2S^2$)
C_p	Specific heat at constant pressure (J/Kg.K)
ρC_p	Heat capacitance of fluid (J/m^3K)
k	Thermal conductivity (J/msK)
t	Time (s)
C	Unsteadiness parameter

Pr	Prandtl number
S	Suction parameter
K	Curvature parameter
R	Radius of curvature (m)
λ_a	Viscous dissipation parameter
e	Dimensionless Curie temperature
β	Ferromagnetic interaction parameter
δ	Dimensionless distance
τ_w	Wall shear stress
q_w	Wall heat flux
C_{fr}	Skin friction coefficient
Nu_L	Local Nusselt number
C_f	Reduced skin friction coefficient
Nu	Reduced local Nusselt number
$f(\eta)$	Dimensionless stream function
$\theta(\eta)$	Dimensionless temperature
$f''(a)$	Skin friction at the wall
$\theta'(a)$	Wall heat transfer gradient
$\varphi'(a)$	Local Sherwood number

Introduction

Biomagnetic fluid mechanics is the study of a certain class of biological problems. Blood flow in the human circulatory system is a well-studied liquid biofluid problem. Diagnosis, surgery and prosthesis are closely related to biomechanics. Different mathematical models, using the principle of fluid

mechanics have been developed with a view to understand the complex phenomena associated with the dynamics of blood flow. These models are currently being used for diagnosis of various arterial diseases, appraisal of newly found treatment procedures like drug delivery and developing and designing various artificial organs. Also, the Navier-Stokes equations could be used to represent blood flow in specific mathematical situations. So, the study of biomagnetic fluid flow is very important not only for understanding of blood flow characteristics through the arteries but also for taking preventive measures of many diseases which occur in the blood vessel.

Basically, biomagnetic fluid dynamics (BFD) is a composition of the principle of ferrohydrodynamics (FHD) and the dominant force in the flow field of magnetohydrodynamics (MHD). Ferrohydrodynamics (FHD) is the mechanics of fluid motion influenced by strong forces of magnetic polarization and in the magnetic field. On the other hand, magnetohydrodynamics (MHD) is the academic discipline concerned with the dynamics of electrically conducting fluids in the presence of a magnetic field. When the magnetization property M_1 is imposed in the magnetic field, then it turned into a biological fluid.

Under the effect of a magnetic fluid, BFD is the investigation of biological fluid. Biomagnetic fluid is known as the fluid which presents in the living creature. Among a number of fluids, blood has the characteristic of biomagnetic fluid. Nowadays, the study of biomagnetic fluid (BFD) is investigated by the number of many researchers for bioengineering and medical applications [1, 2] by controlling blood flow for surgery, cancer treatment, drug targeting [3, 4]. The first mathematical model was developed by Haik et al. [5] for the flow of biomagnetic fluids under the action of an applied magnetic field termed biomagnetic fluid dynamics (BFD) with the principles of ferrohydrodynamics (FHD). Tzirtzilakis [6] developed the electric conductivity along with the polarization and extended BFD model for formulating the entire magnetic features of blood. This model is based on both principles of MHD and FHD and also includes the energy equations. Under the action of a magnetic field, Tzirtzilakis and Kafoussias [7]

analyzed the mathematical model of biomagnetic fluid flow over a linearly stretching sheet which is produced by a magnetic dipole. Khashan and Haik [8] discussed the effect of magnetic field of a magnet on biomagnetic fluid flow downstream of eccentric stenotic orifice, two-dimensionally. Mustapha et al. [9] introduced the effect of uniform magnetohydrodynamic field on blood flow inside an irregular multi-stenosed artery, two-dimensionally and axially symmetric. Abbas et al. [10] developed the hydromagnetic slip flow of nanofluid over a curved stretching surface with heat generation and thermal radiation. In this study, the authors have discussed the flow and heat transfer in a two-dimensional boundary layer flow of an electrically conducting nanofluid over a curved stretching sheet coiled in a circle. Nagaraja and Gireesha [11] have introduced the exponential space depended heat generation impact on MHD convective flow of Casson fluid flow over a curved stretching sheet with chemical reaction. Hayat et al. [12] numerically investigated boundary layer convective flow caused by a nonlinear curved stretching sheet. Also, Hayat et al. [13] analyzed the effects of heterogeneous and homogeneous chemical reactions on non-Newtonian fluids over a curved stretching sheet and found that the strength in heterogeneous reaction increases the concentration of the fluid. Ahmad et al. [14] studied flow over a curved surface embedded in a porous medium and found that the velocity profile flourishes for booming values of curvature parameter. Mathematical models have been developed for blood flow and many researchers like Eldesoky [15] assumed that blood is a Newtonian fluid. Eldesoky [15] studied the MHD blood flow of an unsteady parallel plat in the presence of a heat source. Crane [16] first developed that the shear-driven flow over a stretching sheet constitutes a classical physical problem for a Newtonian fluid. Later, Anderson [17] introduced an exact similarity solution for velocity and pressure of the magnetohydrodynamics flow past a stretching sheet. The study of MHD flow over a stretching sheet still constitutes a topic of current ongoing research. Jat and Chaudhary [18] and Pop et al. [19] developed the radiation effects on the MHD flow near the stagnation point of stretching sheet. In the presence of a transverse magnetic field with heat source/sink, Das et al. [20] proposed the unsteady MHD flow

of nanofluids over an accelerating convectively heated stretching sheet. Under various non-linear stretching velocities, Dandapat et al. [21] introduced the MHD flow of a viscous liquid film over a stretching sheet. In the presence of magnetic field, Misra et al. [22] analyzed the concerned applications of MHD flow problems to hemodynamics of steady incompressible viscoelastic and electrically conducting fluid flow and heat transfer in a parallel plate channel.

Based on the above-mentioned studies, to the authors' knowledge, the numerical study of biomagnetic fluid flow over an unsteady curved stretching sheet in the presence of magnetic field has not been investigated yet. The mathematical model used is that of the extended BFD which incorporates FHD formulations. The extended mathematical model is described by a coupled of nonlinear system of partial differential equations (PDEs). The boundary conditions are considered according to the physical model. The effects of curved geometry are present in the form of the curvature parameter. The numerical solution of the problem is obtained by developing an efficient numerical methodology based on finite difference method with the help of Fortran software. It is hope that the present study will help in understanding the basic mechanism for applications in biomedicine and bioengineering such as separation of targeted molecules, magnetic drug targeting, diagnostic techniques, hyperthermia, or hypothermia treatment, etc.

Mathematical Formulation

Let us consider an unsteady two-dimensional incompressible, viscous, laminar biomagnetic fluid whose flow direction in the coordinate system is taking place in the (s, r) plane and the flow is caused by curved stretching. The sheet is being stretched along a semi-circle of radius R in a two-dimensional frame by two equal and opposite forces applied along the s-direction by keeping the origin fixed, and r-direction is normal to it. We assumed that the sheet is stretched with $U_w(t, s) = \frac{as}{1 - \alpha t}$, where $(a > 0)$

is the stretching constant. The temperature of the stretched sheet is kept fixed at T_w and the temperature of the fluid far away from the sheet is T_∞. The fluid is confined to the half space $(r > 0)$ above the sheet, and magnetic dipole is located at distance d below the sheet, giving rise to a magnetic field of sufficient strength to saturate the biomagnetic fluid. The flow configuration is shown schematically at Figures 1(a) and 1(b).

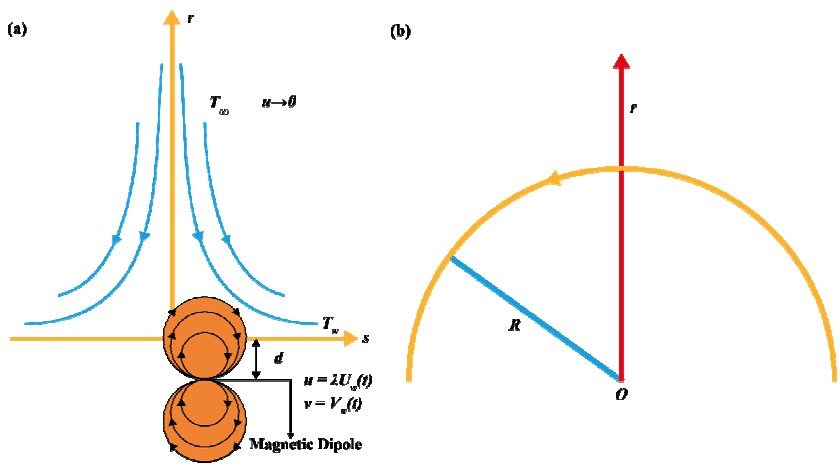

Figure 1. (a) Geometry of the problem for a flat stretching sheet and (b) curved stretching sheet.

The governing equations of the unsteady two-dimensional flow of viscous incompressible biomagnetic fluid and heat transfer equations under the influence of magnetic field are [23]:

$$\frac{\partial}{\partial r}[(r+R)v] + R\frac{\partial u}{\partial s} = 0, \tag{1}$$

$$\frac{u^2}{r+R} = \frac{1}{\rho}\frac{\partial p}{\partial r}, \tag{2}$$

$$\frac{\mu}{\rho}\left[\frac{\partial^2 u}{\partial r^2} + \frac{1}{r+R}\frac{\partial u}{\partial r} - \frac{u}{(r+R)^2}\right]$$
$$= \frac{1}{\rho}\frac{R}{r+R}\frac{\partial p}{\partial s} + \frac{\partial u}{\partial t} + v\frac{\partial u}{\partial r} + \frac{Ru}{r+R}\frac{\partial u}{\partial s} + \frac{uv}{r+R} + \mu_0 M_1\frac{\partial H}{\partial s}, \tag{3}$$

$$\frac{\partial T}{\partial t} + v\frac{\partial T}{\partial r} + \frac{Ru}{r+R}\frac{\partial T}{\partial s}$$

$$= \alpha'\left(\frac{\partial^2 T}{\partial r^2} + \frac{1}{r+R}\frac{\partial T}{\partial r}\right) + \frac{\mu_0 T}{\rho C_p}\frac{\partial M_1}{\partial T}\left(u\frac{\partial H}{\partial s} + v\frac{\partial H}{\partial r}\right), \tag{4}$$

where u and v are the velocity components along s and r directions, respectively, p denotes the pressure, T indicates the temperature of the fluid, C_p is the specific heat at constant pressure, ρC_p is the heat capacitance of fluid, ρ is the mass density, μ is the dynamic viscosity, μ_0 is the magnetic permeability, H is the magnetic field strength, and α' is the thermal diffusivity and denoted by

$$\alpha' = \frac{k}{\rho C_p}.$$

The term $\mu_0 M_1 \frac{\partial H}{\partial s}$ in equation (3) represents the component of the magnetic force per unit volume and depends on the existence of the magnetic gradient in s direction. When the magnetic gradient is absent, this force vanishes. The second term on the right-hand side of the energy equation (4) accounts for heating due to the adiabatic magnetization. These terms are known as FHD [6, 7, 24, 25].

The suitable initial and boundary conditions for the velocity and temperature are [23]:

$$\left.\begin{array}{l} t < 0;\ u = 0,\ v = 0,\ T = T_\infty \text{ for any } r \text{ and } s \\ t \geq 0:\ v = V_w(t),\ u = \lambda U_w(t, s),\ T = T_w \text{ at } r = 0 \\ u \to 0,\ \dfrac{\partial u}{\partial r} \to 0,\ T = T_\infty \text{ as } r \to \infty \end{array}\right\}, \tag{5}$$

where

$$U_w(t, s) = \frac{as}{1-\alpha t} \text{ is the stretching velocity,}$$

$$V_w(t) = -\sqrt{\frac{a\nu t}{1-\alpha t}}S \text{ is the suction velocity.}$$

Here $\lambda < 0$ denotes shrinking and $\lambda > 0$ denotes stretching, where λ is dimensionless constant, $\alpha < 0$ represents decelerated flow and $\alpha > 0$ represents accelerated flow, respectively. $S > 0$ and $S < 0$ give suction and injection, respectively, where S is the constant wall mass transfer parameter. The biomagnetic fluid flow is affected by the magnetic field generated by the presence of a magnetic dipole. It is assumed that the magnetic dipole is located at distance d below the sheet. The magnetic dipole gives rise to a magnetic field, sufficiently strong to saturate the fluid and its scalar potential whose components $H_{\bar{x}}$ and $H_{\bar{r}}$ of the magnetic field $\vec{H} = (H_{\bar{x}}, H_{\bar{r}})$, due to magnetic dipole, are given by [6, 7, 26, 27]:

$$H_s(s, r) = -\frac{\partial V}{\partial s} = \frac{\gamma}{2\pi}\frac{s^2 - (r+d)^2}{[s^2 + (r+d)^2]^2},$$

$$H(s, r) = \frac{\gamma}{2\pi}\left[\frac{1}{(r+d)^2} - \frac{s^2}{(r+d)^4}\right],$$

$$H(0, 0) = \frac{\gamma}{2\pi}\left[\frac{1}{(0+d)^2} - \frac{0^2}{(0+d)^4}\right] = \frac{\gamma}{2\pi}\frac{1}{d^2},$$

Thus

$$\frac{\partial H}{\partial s} = \frac{\gamma}{2\pi}\frac{-2s}{(r+d)^4},$$

$$\frac{\partial H}{\partial r} = \frac{\gamma}{2\pi}\frac{-2}{(r+d)^3} + \frac{4s^2}{(r+d)^5}.$$

Moreover, under the assumption that the applied magnetic field H is sufficiently strong to saturate the biomagnetic fluid, the magnetization M_1 is generally determined by the fluid temperature and magnetic field intensity H. There is a variety of equations that can be used for the variation of the magnetization under the equilibrium assumption. In this study, the adopted relation expresses the magnetization M_1 as a function of temperature T and

magnetic field intensity H, given by $M_1 = K_1 H(T_\infty - T)$, where K_1 is a constant known as pyromagnetic coefficient and T_∞ is the Curie temperature [28]. The above relation for the magnetization M_1 has also proposed for the formulation of BFD [29].

Following variables are used for nondimensionalizing [23] the system of differential equations (1)-(4) with boundary condition (5):

$$\left.\begin{aligned} &\eta = \sqrt{\frac{a}{\nu(1-\alpha t)}}\, r,\ v = -\frac{R}{r+R}\sqrt{\frac{a\nu}{1-\alpha t}}\, f(\eta),\ u = \frac{as}{1-\alpha t} f'(\eta) \text{ for } \alpha \le 0 \\ &p = \frac{\rho a^2 s^2}{(1-\alpha t)^2} P(\eta) \\ &\theta(\eta) = \frac{T_\infty - T}{T_\infty - T_w} \end{aligned}\right\}, \tag{6}$$

where $\theta(\eta)$ is the dimensionless temperature function, $f(\eta)$ is the dimensionless velocity function, η is the dimensionless similarity variable, prime denotes derivative with respect to η, T_∞ is the embedded temperature and T_w is the surface temperature, $K = \sqrt{\frac{a}{[\nu(1-\alpha t)]}}\, R$ denotes the curvature parameter. Also, the continuity equation (1) is satisfied using the similarity variables (6).

Substituting (6) into (1)-(4), we get

$$\frac{\partial P}{\partial \eta} = \frac{1}{K+\eta} f'^2, \tag{7}$$

$$\begin{aligned} \frac{2K}{K+\eta} P = {} & f''' + \frac{1}{\eta + K} f'' - \frac{1}{(\eta+K)^2} f' \\ & + \left[\frac{K}{K+\eta} f f'' - \frac{K}{K+\eta} f'^2 + \frac{K}{(K+\eta)^2} f f' - C\left(f' + \frac{\eta}{2} f''\right)\right] \\ & + \frac{2\beta\delta^2\theta}{(\eta+\delta)^6}, \end{aligned} \tag{8}$$

$$\theta'' + \frac{1}{\eta + K}\theta' = Pr\left(\frac{C\eta}{2}\theta' - \frac{K}{\eta + K} f\theta'\right) - \frac{2\beta\delta^4}{(\eta + \delta)^5}\frac{K}{\eta + K}\lambda_a(e - \theta). \quad (9)$$

The associated boundary conditions are:

$$f(0) = S, \quad f'(0) = \lambda, \quad \theta(0) = 1, \quad (10)$$

$$f'(\eta) \to 0, \quad f''(\eta) \to 0, \quad \theta(\eta) \to 0 \text{ as } \eta \to \infty, \quad (11)$$

where $K = R\sqrt{\frac{a}{\nu(1 - \alpha t)}}$ is the curvature parameter, $C = \frac{\alpha}{a}$ is unsteadiness parameter, $Pr = \frac{\nu}{\alpha'}$ is the Prandtl number, $e = \frac{T_\infty}{T_\infty - T_w}$ is the dimensionless temperature parameter, $\lambda_a = \frac{\mu^3}{k\rho^2(T_\infty - T_w)d^2}$ is the viscous dissipation parameter, $\delta = \sqrt{\frac{a}{\nu(1 - \alpha t)}}d$ is the dimensionless distance and $\beta = \frac{\gamma}{2\pi}\frac{\mu_0 K_1 H(0, 0)(T_\infty - T_w)\rho}{\mu^2}$ is the ferromagnetic interaction parameter.

The important physical characteristics skin friction coefficient C_{fr} and local Nusselt number Nu_L are described by

$$C_{fr} = \frac{\tau_w}{\rho(as)^2} \quad \text{and} \quad Nu_L = \frac{sq_w}{k(T_w - T_\infty)}, \quad (12)$$

where τ_w is the local shear stress at wall, while q_w represents the heat transfer from the sheet, given by

$$\tau_w = \mu\left(\frac{\partial u}{\partial r} - \frac{u}{r + R}\right)_{r=0} \quad \text{and} \quad q_w = -k\left(\frac{\partial T}{\partial r}\right)_{r=0}. \quad (13)$$

Introducing (13) into (12), the skin friction coefficient and local Nusselt number can be written in dimensionless form as

$$C_f = f''(0) - \frac{\lambda}{k} \quad \text{and} \quad Nu = -\theta'(0), \quad (14)$$

where $C_f = Re_s^{\frac{1}{2}}(1-\alpha t)^{\frac{3}{2}} C_{fr}$ is the reduced skin friction coefficient, $Nu = (Re_s)^{\frac{-1}{2}}(1-\alpha t)^{\frac{1}{2}} Nu_L$ signifies reduced local Nusselt number and $Re_s = \frac{as^2}{\nu}$ represents the local Reynolds number.

Numerical Procedure

We have described a simple and efficient approximate numerical technique to obtain the numerical solution of two-point boundary value problems under consideration. The base of this numerical technique is the common finite difference method with central differencing, a tridiagonal matrix manipulation and an iterative procedure. This numerical method is described in detail in Kafoussias and Williams [30]. The entire numerical method is accurate, stable and instantaneously converging. In fluid mechanics, it is an accurate and powerful method which is appropriate for application to a wide class of two-point boundary value similarity problems [29]. So, we can apply it easily.

The momentum equation (8) is highly nonlinear with the boundary conditions (10) and (11). By reducing the momentum equation (8) to a second order linear differential equation by assuming:

$$F(x) = f'(\eta), \quad F'(x) = f''(\eta), \quad F''(x) = f'''(\eta),$$

the momentum equation (8) can be written as

$$F''(x) + \left[\frac{1}{K+\eta} + \frac{K}{K+\eta} f - \frac{\eta}{2} C\right] F'(x)$$

$$- \left[\frac{1}{(K+\eta)^2} + \frac{K}{K+\eta} f' - \frac{K}{(K+\eta)^2} f + C\right] F(x)$$

$$= \frac{2K}{K+\eta} P - \frac{2\beta\delta^2\rho_\theta}{(\eta+\delta)^6} \tag{15}$$

which is of the form

$$P(x)F''(x) + Q(x)F'(x) + R(x)F(x) = S(x), \tag{16}$$

where

$$P(x) = 1,\ Q(x) = \frac{1}{K+\eta} + \frac{K}{K+\eta} f - \frac{\eta}{2} C,$$

$$R(x) = -\left[\frac{1}{(K+\eta)^2} + \frac{K}{K+\eta} f' - \frac{K}{(K+\eta)^2} f + C\right],$$

$$S(x) = \frac{2K}{K+\eta} P - \frac{2\beta\delta^2\rho_\theta}{(\eta+\delta)^6}.$$

By using a common finite difference method which is based on central differencing and tridiagonal matrix manipulation, equation (16) can be solved. To start the solution procedure, we assume initial guesses for $f'(\eta)$ between $\eta = a$ and $\eta = \eta_\infty$ $(\eta_\infty \to \infty)$ which should obviously satisfy the boundary conditions (10) and (11). For the present problem, we insert the following initial guesses:

$$f(\eta) = S - \frac{\eta}{\eta_\infty}, \quad f'(\eta) = \lambda - \frac{\eta}{\eta_\infty}, \quad \theta(\eta) = 1 - \frac{\eta}{\eta_\infty}.$$

The function $f(\eta)$ is obtained by integrating the curve $f'(\eta)$. To propose a new estimation for $f'(\eta)$ and $f'_{new}(\eta)$, we have to consider the functions f and θ. The next step is to solve the non-linear equation (16) by using the above method. We have obtained the updated value of $f(\eta)$ by integrating the curve $f'_{new}(\eta)$.

These new profiles of $f'(\eta)$ and $f(\eta)$ are then imposed for getting new inputs and so on. In this scheme, the momentum equation (8) is solved iteratively until convergence up to a small quantity $|f''_{new} - f''| \le \varepsilon_1$ is obtained.

After obtaining the function $f(\eta)$, the solution of the energy equation (9) with boundary conditions (10) and (11) is solved by using the same algorithm, but without iteration as equation (9) is linear.

Now, the energy equation (9) can be re-written as

$$\theta'' + \left[\frac{1}{\eta + K} - Pr\left(\frac{C\eta}{2} - \frac{K}{K + \eta} f\right)\right]\theta' - \frac{2\beta\delta^4}{(\eta + \delta)^5}\frac{K}{\eta + K}\lambda_a\theta$$

$$= \frac{2\beta\delta^4}{(\eta + \delta)^5}\frac{K}{\eta + K}\lambda_a T_\varepsilon. \tag{17}$$

In this way, we get a new approximation θ_{new} for θ by considering $f(\eta)$, $f'(\eta)$. This process is continuing until convergence up to a small quantity $|\theta'_{new} - \theta'| \leq \varepsilon_1$ is obtained and finally we obtain θ.

In order to apply to our numerical computation, a proper step size $h = \Delta\eta = 0.01$ and appropriate $\eta_{\max}$ value must be determined. By "trial and error", we set $\eta_{\min} = 0.1$, $\eta_{\max} = 10$ and the tolerance between the iterations is set at $\varepsilon_1 = 10^{-4}$ defined as $\varepsilon_1 = \max_{i=1,N}\left(\left|\frac{f_{old}(i) - f_{new}(i)}{f_{old}(i)}\right|\right)$. Computations were also performed for $\Delta\eta = 0.001$ and no significant differences were found.

Numerical Validation

In order to establish the validity and accuracy of the method, we have computed the skin friction coefficient with $S = 0$, $\lambda = 1$, $\lambda_1 = 0$, $\beta = 0$, $\phi = 0$ for the values of curvature parameter $K =$ 5, 10, 15, 20, 25, 30, 35, 40, 45, 50 and compared with those reported by Usama et al. [23] which is shown in Table 1. This observation serves as a confirmation of the accuracy of the results and shows an excellent agreement, see Table 1.

Table 1. Comparison of skin friction coefficients $-f''(0)$ for different values of curvature parameter with specific values of $S = 0$, $\lambda = 1$, $\lambda_1 = 0$, $\beta = 0$, $\phi = 0$

K	Usama et al. [23]	Present
5	1.1648	1.1654
10	1.07659	1.0758
15	1.05001	1.0505
20	1.03722	1.0370
25	1.0297	1.0297
30	1.02475	1.0250
35	1.02124	1.0263
40	1.01863	1.0272
45	1.01661	1.0280
50	1.01499	1.0286

Results and Discussion

In order to get the numerical solution, it is necessary to determine some specific values for the dimensionless parameters involved in the problem under consideration. It is noted that most of the fluids like human blood, the body temperature is considered as $T_w = 37^\circ\text{C} = 310^\circ\text{K}$ and the body Curie temperature is $T_\infty = 41^\circ\text{C} = 314^\circ\text{K}$ [31]. For the above values, it is obtained that the dimensionless temperature $e = 78.5$ [31], viscous dissipation parameter $\lambda_a = 6.4 \times 10^{-14}$ [31] and dimensionless distance $\delta = 1$ [7, 25]. Moreover, the values of the leading parameters were as follows: the Prandtl number $Pr = 17, 21, 23, 25$ [32, 33], ferromagnetic interaction parameter $\beta = 0, 5, 10$ [11, 31, 34], curvature parameter $K = 1$, 2, 3, 5, 10, 15, 20, 50, 100, 500 [11, 23, 35], Suction parameter $S = 1, 2, 3, 4$ [23, 36], stretching parameter $\lambda = 1, 1.5, 2$ [23] and unsteadiness parameter $C = 0, 0.1, 0.2, 0.3, 0.5, 0.8, 1, 1.5$ [37].

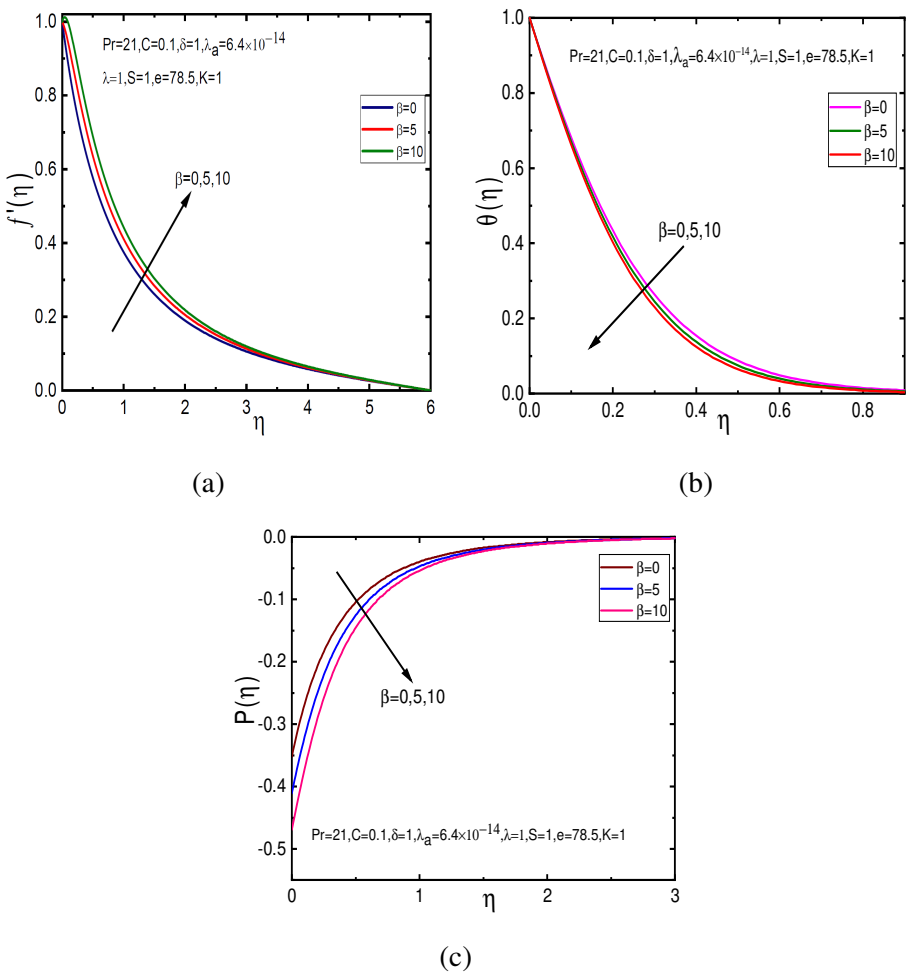

Figure 2. (a) Velocity, (b) temperature and (c) pressure profiles for different values of β.

The function $f'(\eta)$ is called *dimensionless velocity component*, $\theta(\eta)$ is called *dimensionless temperature* and $P(\eta)$ is called *dimensionless pressure*. The curves (Figures 2(a)-2(c)) are plotted for $M = 0$ and $\beta = 0, 5, 10$ which correspond to FHD flow of the extended BFD model. Figure 2 demonstrates the velocity profile, the temperature profile and dimensionless pressure for numerous values of ferromagnetic interaction

parameter β. Figure 2(a) shows the effect of ferromagnetic interaction parameter β on the velocity profile. Here it is observed that when the value of ferromagnetic interaction parameter β increases, then the velocity profile increases whereas reverse trend is found for temperature profile and dimensionless pressure as shown in Figure 2(b) and 2(c).

Figure 3 shows the effect of curvature parameter K on the velocity, temperature and dimensionless pressure profiles. The velocity and temperature profiles for various values of curvature parameter K are shown in Figures 3(a) and 3(b). In this case, it is noticed that the velocity and heat transfer are gradually decreased with the increment of K. This is because an increase in K tends to make the surface more flat which results into the decrease of velocity and temperature profiles. The effect of curvature parameter K on the dimensionless pressure is shown in Figure 3(c) for $K =$ 1, 5, 20, 50 and 500. This figure indicates that magnitude of pressure inside the boundary layer is increased as dimensionless curvature parameter is increased. However, the pressure approaches zero far from the boundary. Because the stream lines of the flow treat in the similar way as they operate in the flow past a flat stretching sheet as we turn away from the boundary. The magnitude of the pressure is an increasing function of the dimensionless curvature at the surface of the stretching sheet. However, the variation of pressure is very important in the case of a curved sheet inside the boundary layer. So, the variation of pressure cannot be neglected as is usually done for a flat stretching sheet.

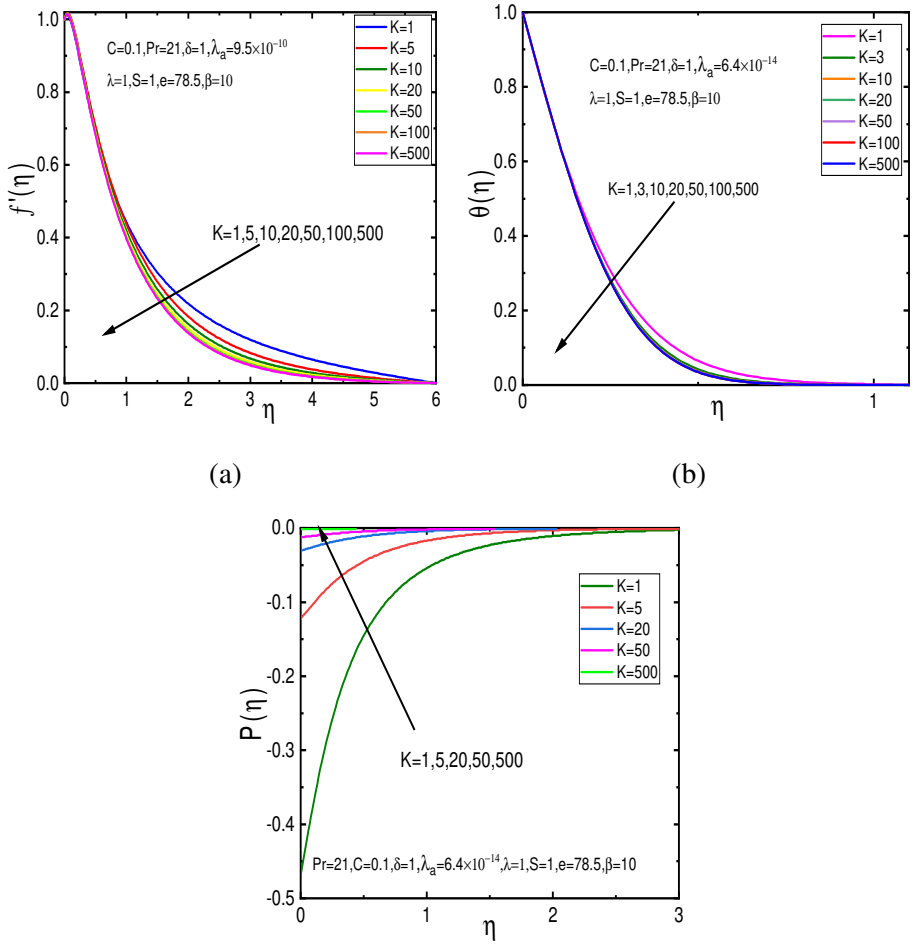

Figure 3. (a) Velocity, (b) temperature and (c) pressure profiles for different values of *K*.

Figure 4 shows the effect of Prandtl number *Pr* on the temperature profile $\theta(\eta)$. Here, it is noticed that the temperature profile $\theta(\eta)$ decreases as Prandtl number *Pr* increases. Moreover, as the Prandtl number increases, the thermal boundary layer thickness decreases. This figure shows that by increasing Prandtl number, the temperature gradient at the surface

also increases. When fluid particularly for blood acquires a higher Prandtl number, its thermal conductivity decreases downward and so that heat conduction capacity decreased.

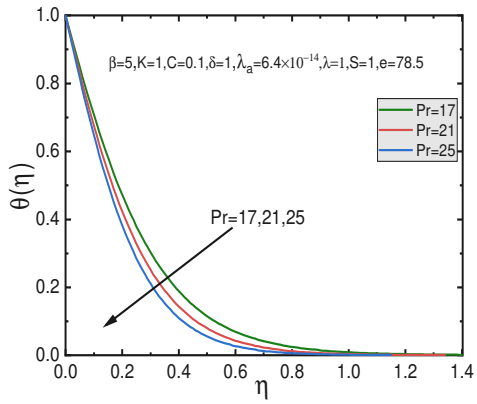

Figure 4. Temperature profile for different values of *Pr*.

Figure 5 demonstrates the velocity, temperature and dimensionless pressure profiles for various values of stretching parameter $\lambda(>0)$ for accelerated flow. From Figure 5(a), we can observe that the velocity profile is increased with the increment of the stretching parameter λ. This is caused due to the opposite directions of stretching and free stream velocities. Figures 5(b) and 5(c) illustrate the effect of stretching parameter $\lambda(>0)$ for accelerated flow on the temperature profile and dimensionless pressure. The temperature profile and dimensionless pressure are decreased with the increment of the stretching parameter λ.

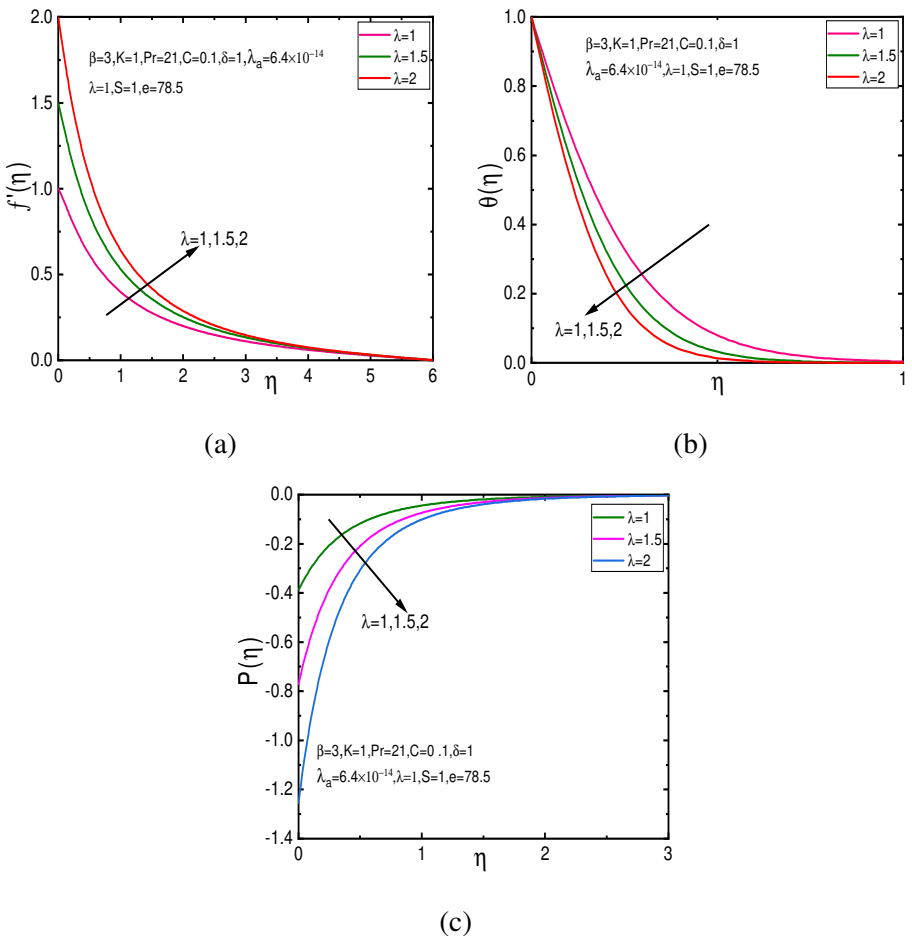

Figure 5. (a) Velocity, (b) temperature and (c) pressure profiles for different values of λ.

Figure 6 demonstrates the velocity, temperature and dimensionless pressure for various values of suction parameter S. Figure 6(a) shows the velocity profile for various values of suction parameter S. It is apparent that the dimensionless velocity profile reduces with the increment of S. This is happened because the suction takes away the arrogant fluid from the surface of the sheet. Figure 6(b) shows the variation of temperature profile with suction parameter S. It is observed that the temperature profile in the flow region reduces as suction parameter increases. This happens because suction

parameter enhances taking away more arrogant fluid from the fluid region causing depreciation in thermal boundary layer thickness. Figure 6(c) shows the variation of the dimensionless pressure with suction parameter *S*. It is apparent that the dimensionless pressure increases linearly with the increment of *S*.

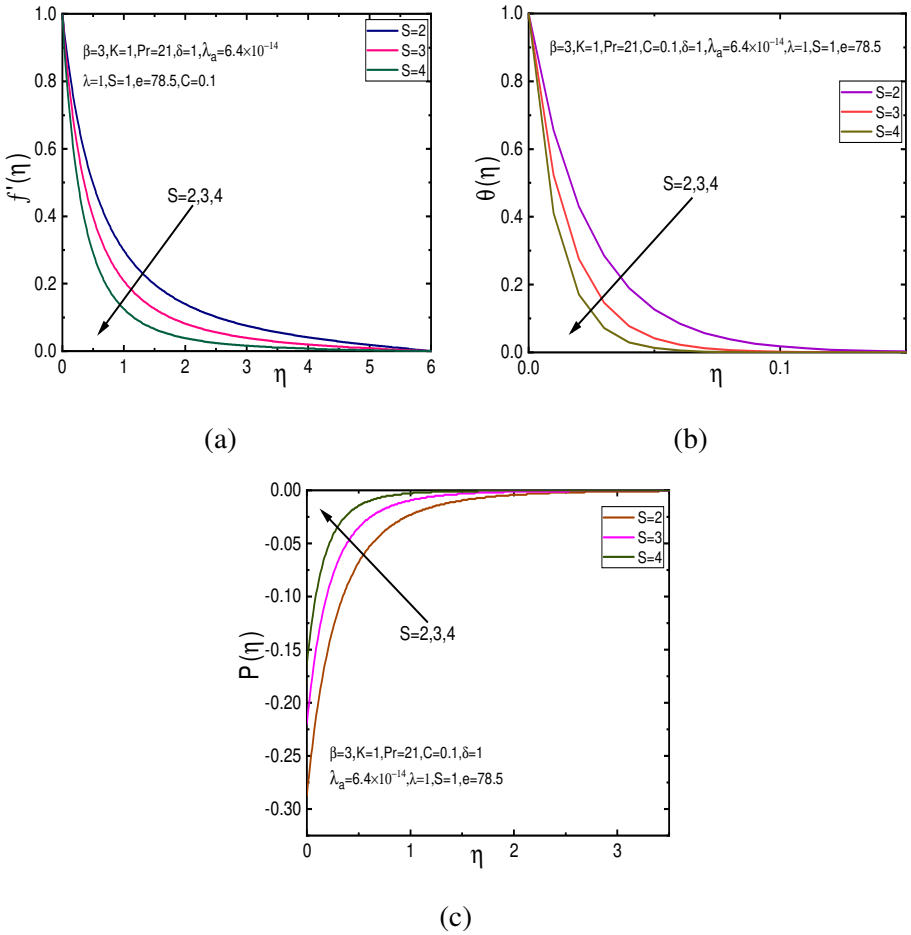

Figure 6. (a) Velocity, (b) temperature and (c) pressure profiles for different values of λ.

Figures 7(a) and 7(b) exhibit the variation of skin friction coefficient and rate of heat transfer as a function of ferromagnetic interaction parameter with different values of *Pr*. From these figures, we observed that skin

friction coefficient is increased with the increasing value of *Pr* whereas rate of heat transfer shows the transverse relation.

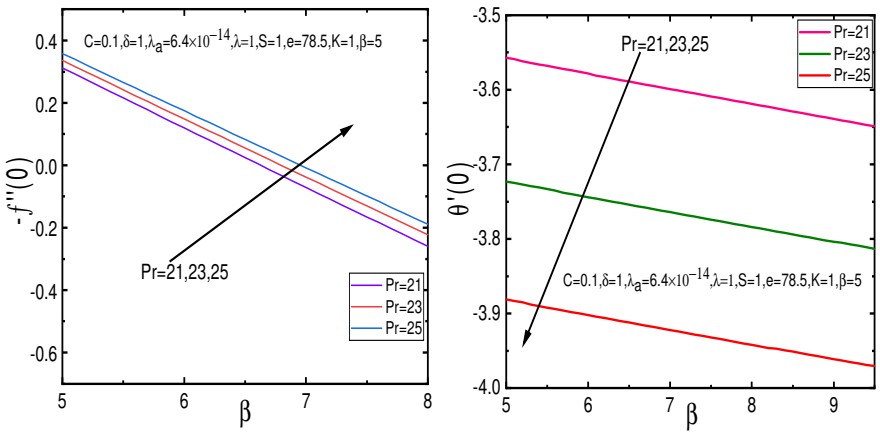

(a) (b)

Figure 7. Variation of (a) skin friction coefficient and (b) rate of heat transfer with various values of *Pr*.

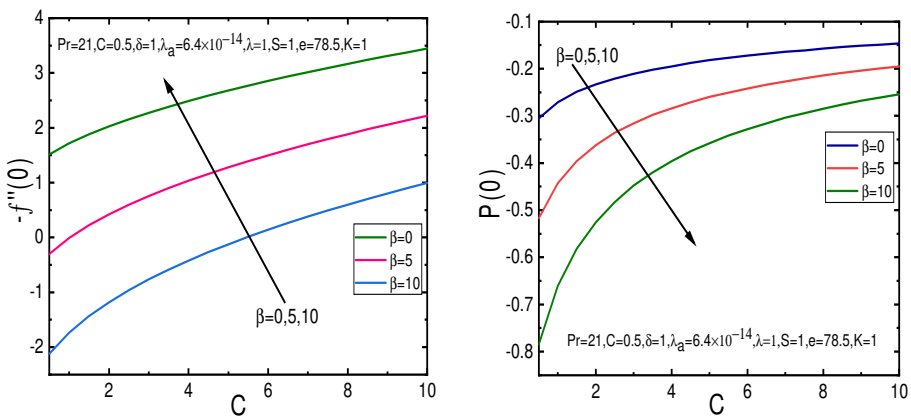

(a) (b)

Figure 8. Variation of (a) skin friction coefficient and (b) dimensionless wall pressure with various values of β.

Figures 8(a) and 8(b) illustrate the variation of skin friction coefficient and dimensionless wall pressure as a function of unsteadiness parameter

with different values of β. These figures show that the skin friction coefficient is increased with the increasing value of β while reverse trend is found for dimensionless wall pressure.

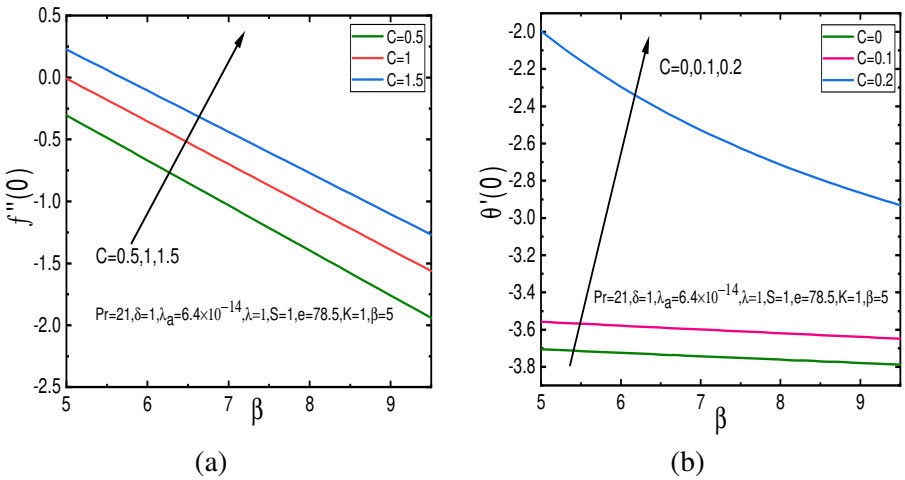

(a) (b)

Figure 9. Variation of (a) skin friction coefficient and (b) rate of heat transfer with various values of *C*.

Figures 9(a) and 9(b) represent the variation of skin friction coefficient and rate of heat transfer as a function of ferromagnetic interaction parameter with different values of *C*. From the figures, we observed that as the unsteadiness parameter increases, then the skin friction coefficient and heat transfer rate at the surface increase.

Conclusion

On the basis of the computational results, we can draw the following conclusions:

❖ The ferromagnetic parameter has a dominating control over the flow of the biomagnetic fluid and heat transfer.

❖ Fluid velocity increases with the increasing value of ferromagnetic and stretching parameters whereas reverse trend is found for temperature and pressure profiles.

❖ The velocity profile is decreased with the increment of unsteadiness parameter whereas temperature and dimensionless pressure profiles show inverse relation.

❖ By increasing the value of Prandtl number, the temperature distributions decrease.

❖ Both velocity and temperature profiles decrease with the increasing value of curvature and suction parameters whereas reverse trend is found for dimensionless pressure.

❖ The skin friction coefficient increases with the increment of K against β and decreases in terms of C whereas the rate of heat transfer and wall pressure increase with the increment of K against β, C and Pr.

❖ The skin friction coefficient decreases with the increment of β against K and Pr and increases in terms of C whereas the rate of heat transfer and wall pressure decrease against K, C and Pr.

❖ The skin friction coefficient, rate of heat transfer and wall pressure increase with the increment of unsteadiness parameter C.

It is hope that the present study will help in understanding the basic mechanism for applications in biomedicine and bioengineering such as separation of targeted molecules, magnetic drug targeting, diagnostic techniques, hyperthermia, or hypothermia treatment, etc.

References

[1] A. N. Rusetski and E. K. Ruuge, Magnetic fluids as drug carriers: targeted transport of drugs by a magnetic field, Journal of Magnetism and Magnetic Materials 122 (1999), 335-339.

[2] M. Lauva and J. Plavins, Study of colloidal magnetite binding erythrocytes: prospects for cell separation, Journal of Magnetism and Magnetic Materials 122 (1993), 349-353.

[3] A. Gul, E. E. Tzirtzilakis and S. S. Makhanov, Simulation of targeted magnetic drug delivery: two-way coupled biomagnetic fluid dynamics approach, Phys. Fluids 34(2) (2022), 021911.

[4] S. A. Jumana, M. Ferdows and E. E. Tzirtzilakis, Biomagnetic flow of heat transfer over moving horizontal plate by the presence of variable viscosity and temperature, Journal of Mechanics in Medicine and Biology 22 (2022), 2250063. https://doi.org/10.1142/S0219519422500634.

[5] Y. Haik, J. C. Chen and V. M. Pai, Development of biomagnetic fluid dynamics, Proceedings of the IX International Symposium on Transport Properties in Thermal Fluid Engineering, Singapore, 1996.

[6] E. E. Tzirtzilakis, A mathematical model for blood flow in magnetic field, Phys. Fluids 17(7) (2005), 077103-077114. https://doi.org/10.1063/1.1978807.

[7] E. E. Tzirtzilakis and N. G. Kafoussias, Biomagnetic fluid flow over a stretching sheet with nonlinear temperature dependent magnetization, Z. Angew. Math. Phys. (ZAMP) 54(4) (2003), 551-565.

[8] S. A. Khashan and Y. Haik, Numerical simulation of biomagnetic fluid downstream an eccentric stenotic orifice, Phys. Fluid 18 (2006), 113601.

[9] N. Mustapha, N. Amin, S. Chakravarty and P. K. Mandal, Unsteady magnetohydrodynamics blood flow through irregular multi-stenosed arteries, Computer in Biology and Medicine 39(10) (2009), 896-906.

[10] Z. Abbas, M. Naveed and M. Sajid, Hydromagnetic slip flow of nanofluid over a curved stretching surface with heat generation and thermal radiation, Journal of Molecular Liquids 215 (2016), 756-762.

[11] B. Nagaraja and B. J. Gireesha, Exponential apace-dependent heat generation impact on MHD convective flow of Casson fluid over a curved stretching sheet with chemical reaction, Journal of Thermal Analysis and Calorimetry 143(6) (2021), 4071-4079.

[12] T. Hayat, R. S. Saif, R. Ellahi, T. Muhammad and B. Ahmad, Numerical study of boundary-layer flow due to a nonlinear curved stretching sheet with convective heat and mass conditions, Results Physics 7 (2017), 2601-2606.

[13] T. Hayat, S. Ayub and A. Alsaedi, Homogeneous-heterogeneous reactions in curved channel with porous medium, Results Physics 9 (2018), 1455-1461.

[14] S. Ahmad, S. Nadeem and N. Muhammad, Boundary layer flow over a curved surface imbedded in porous medium, Communications in Theoretical Physics 71(3) (2019), 344-348.

[15] M. I. Eldesoky, Mathematical analysis of unsteady MHD blood flow through parallel plate channel with heat source, World Journal of Mechanics 2 (2012), 131-137.

[16] L. J. Crane, Flow past a stretching plate, J. Appl. Math. Phys. (ZAMP) 21 (1970), 645-647.

[17] H. I. Anderson, An exact solution of the Navier-Stokes equations for magneto-hydrodynamics flow, Acta. Mech. 113 (1995), 241-244.

[18] R. N. Jat and S. Chaudhary, Radiation effects on the MHD flow near the stagnation point of a stretching sheet, Z. Angew. Math. Phys. 61 (2010), 1151-1154.

[19] I. Pop, A. Ishak and F. Aman, Radiation effects on the MHD flow near the stagnation point of a stretching sheet: revisited, Z. Angew. Math. Phys. 62 (2011), 953-956.

[20] S. Das, S. Chakraborty, R. N. Jana and O. D. Makinde, Entropy analysis of unsteady magneto-nanofluid flow past accelerating stretching sheet with convective boundary condition, Appl. Math. Mech. (Engl. Ed.) 36(12) (2015), 1593-1610.

[21] B. S. Dandapat, B. Santra and S. K. Singh, Thin film flow over a non-linear stretching sheet in presence of uniform transverse magnetic field, Z. Angew. Math. Phys. 61 (2010), 685-695.

[22] J. C. Misra, G. C. Shit and H. J. Rath, Flow and heat transfer of a MHD viscoelastic fluid in a channel with stretching walls: some applications to haemodynamics, Comput. Fluids 37(1) (2008), 1-11.

[23] Usama, S. Nadeem and A. U. Khan, Stability analysis of Cu-H_2O nanofluid over a curved stretching/shrinking sheet: Existence of dual solutions, Canadian Journal of Physics 97(8) (2019), 911-922.

[24] R. E. Rosensweig, Magnetic fluids, Annual Review of Fluid Mechanics 19 (1987), 437-461.

[25] M. Ramzan, N. S. Khan and P. Kumam, Mechanical analysis of non Newtonian nanofluid past a thin needle with dipole effect and entropic characteristics, Scientific Reports 11(1) (2021), 1-25.

[26] H. I. Andersson and O. A. Valnes, Flow of a heated ferrofluid over a stretching sheet in the presence of a magnetic dipole, Acta Mechanica 128(1) (1998), 39-47.

[27] E. E. Tzirtzilakis and G. B. Tanoudis, Numerical study of biomagnetic fluid flow over a stretching sheet with heat transfer, International Journal of Numerical Methods for Heat and Fluid Flow 13(3) (2003), 830-848.
doi: 10.1108/09615530310502055.

[28] H. Matsuki, K. Yamasawa and K. Murakami, Experimental considerations on a new automatic cooling device using temperature sensitive magnetic fluid, IEEE Transaction on Magnetics 13(5) (1977), 1143-1145.

[29] E. E. Tzirtzilakis and N. G. Kafoussias, Three-dimensional magnetic fluid boundary layer flow over a linearly stretching sheet, Journal of Heat Transfer 132(1) (2010), 011702. https://doi.org/10.1115/1.3194765.

[30] N. G. Kafoussias and E. W. Williams, An improved approximation technique to obtain numerical solution of a class of two-point boundary value similarity problems in fluid mechanics, Internat. J. Numer. Methods Fluids 17(2) (1993), 145-162.

[31] M. G. Murtaza, E. E. Tzirtzilakis and M. Ferdows, Effect of electrical conductivity and magnetization on biomagnetic fluid flows over a stretching sheet, Z. Angew. Math. Phys. 68(4) (2017), 1-15.

[32] J. Alam, M. G. Murtaza, E. E. Tzirtzilakis and M. Ferdows, Application of biomagnetic fluid dynamics modeling for simulation of flow with magnetic particles and variable fluid properties over a stretching cylinder, Math. Comput. Simulation 199 (2022), 438-462.

[33] E. E. Tzirtzilakis, A simple numerical methodology for BFD problems using stream function vortices formulation, Comm. Numer. Methods Engrg. 24 (2008), 683-700.

[34] M. G. Murtaza, E. E. Tzirtzilakis and M. Ferdows, Biomagnetic fluid flow past a stretching/shrinking sheet with slip conditions using lie group analysis, AIP Conf. Proc. 2121, 2019, 050005.

[35] M. Sajid, N. Ali, T. Javed and Z. Abbas, Stretching a curved surface in a viscous fluid, Chinese Physics Letters 27 (2010), 024703.

[36] M. Ferdows, G. Murtaza, J. C. Misra and E. E. Tzirtzilakis, Dual solutions in biomagnetic fluid flow and heat transfer over a nonlinear stretching/shrinking: application of lie group transformation, Math. Biosci. Eng. 17(5) (2020), 4852-4874.

[37] M. G. Murtaza, E. E. Tzirtzilakis and M. Ferdows, Numerical solution of three dimensional unsteady biomagnetic flow and heat transfer through stretching/shrinking sheet using temperature dependent magnetization, Archives of Mechanics 70(2) (2018), 161-185.